

Semi-Supervised Audio-Visual Video Action Recognition with Audio Source Localization Guided Mixup

Seokun Kang, Taehwan Kim
Artificial Intelligence Graduate School
Ulsan National Institute of Science & Technology
{oraclemiso, taehwankim}@unist.ac.kr

Abstract

Video action recognition is a challenging but important task for understanding and discovering what the video does. However, acquiring annotations for a video is costly, and semi-supervised learning (SSL) has been studied to improve performance even with a small number of labeled data in the task. Prior studies for semi-supervised video action recognition have mostly focused on using single modality - visuals - but the video is multi-modal, so utilizing both visuals and audio would be desirable and improve performance further, which has not been explored well. Therefore, we propose audio-visual SSL for video action recognition, which uses both visual and audio together, even with quite a few labeled data, which is challenging. In addition, to maximize the information of audio and video, we propose a novel audio source localization-guided mixup method that considers inter-modal relations between video and audio modalities. In experiments on UCF-51, Kinetics-400, and VGGSound datasets, our model shows the superior performance of the proposed semi-supervised audio-visual action recognition framework and audio source localization-guided mixup.

1. Introduction

Video is considered an important resource for deep learning vision research. Video data of different lengths and formats has become more readily available as large-scale video content offerings and user interactions on online platforms increase. This leads to active research on video understanding [23, 24, 26, 44] and among them, video action recognition is one of the challenging tasks [8, 14, 22, 36, 52, 56].

Unlike image classification, video action recognition is a challenging task that requires understanding both spatial and temporal information. This requires sufficient labeled training data, but labeling on video data is more difficult and time-consuming than images. Nevertheless, unlabeled video data is readily available, and semi-supervised learning (SSL) methods using labeled video and large-scale unlabeled video together are being actively studied [43, 48, 49, 51].

Semi-supervised video action recognition research remains less explored compared to semi-supervised image classification [6, 9, 38, 46, 54]. Recent studies in SSL video recognition have actively explored various approaches beyond just using fixed, flexible, or even not predefined confidence-based thresholds [38, 46, 54] as proposed in the SSL image domain. These include leveraging pre-trained networks and large-scale unlabeled datasets [11, 18, 49]. In addition, research efforts are increasingly focusing on the utilization of additional modalities such as temporal gradient [48] and optical flow [50] obtained from video data or by introducing auxiliary networks [51].

Studies of semi-supervised learning for image and video use random augmentation techniques to generate weak and strong augmented images or videos and train the model through consistency regularization using both augmented [38, 46, 49, 51, 54]. In this context, weak augmentations typically involve random flips and rotations, while strong augmentations utilize RandAugment [10] that includes techniques such as CutMix [53], which involves cutting and combining different images, and MixUp [55], which mixes images through interpolation.

However, SVFormer [49] points out the limitations of mixup and cutmix that do not produce the expected performance in the video domain, and to overcome these limitations, they propose TubeToken Mixup and Temporary Warping augmentation methods. However, there is still a limitation in that they cannot actively utilize all its information because only visual information is considered, not audio information. In semi-supervised video action recognition, using visual-audio modality has been under-explored. The only exception is AvCLR [3], which employs audio-visual contrastive learning with ResNet architecture. However, despite originating from the same video clip, augmentations for video and audio modalities are conducted indi-

vidually without profoundly considering the inter-modal relation between these modalities.

In this paper, we propose the transformer-based framework for semi-supervised audio-visual action recognition with audio source localization-guided mixup. Specifically, we introduce a novel audio source localization-guided mixup method designed to preserve the inter-modal relations that tend to be overlooked when applying mixup or cutmix to visual and audio modalities. In most cases, visual and audio information occur simultaneously and are interrelated in videos. By preserving this inter-relationship within videos, models can better understand and reflect real-world situations.

In addition, we leverage contrastive learning between video and audio modalities in the video clip. Incorporating audio source localization guided mixup with contrastive learning can improve performance substantially over existing state-of-the-art methods.

In summary, our contributions are as follows:

- We study semi-supervised audio-visual action recognition, which has been under-explored. To the best of our knowledge, we propose, for the first time, a visual-audio semi-supervised video action recognition approach based on the transformer model. This allows for the maximization of the use of visual and audio information inherent in videos.
- We propose a novel audio source localization-guided mixup that, unlike mixup or cutmix, preserves the interrelation between the video and audio modalities.
- In experiments, our proposed model outperforms the existing state-of-the-art model on three different benchmark datasets in even challenging scenarios with only a few labeled samples available.

2. Related Works

2.1. Semi-supervised Image Classification

Deep learning-based image classification has achieved significant performance improvements by leveraging large-scale annotated datasets [13, 15, 16, 20, 27, 41]. However, annotating requires considerable time and resources. To address this, semi-supervised learning (SSL) methods, which use a few labeled datasets and large-scale unlabeled datasets, have been introduced. These approaches aim to reduce annotating time and resource consumption while improving performance. The most commonly used techniques include consistency learning through data augmentations [4, 42] and the use of pseudo labels [12, 21]. Consistency learning focuses on training the model to make consistent predictions about augmented images, while pseudo-labeling uses the model’s predictions on unlabeled data as pseudo-labels. Additionally, various studies use consistency learning and pseudo-labeling together to reduce bias from pseudo-label

via a thresholding approach. For example, FixMatch [38] uses fixed predefined thresholds, FlexMatch [54] employs flexible thresholds, and FreeMatch [46] uses thresholds that are not predefined but are also flexible.

2.2. Semi-supervised Video Recognition

As the creation and utilization of video data increase across various platforms, research on video understanding is becoming increasingly active [11, 23, 24, 26, 44]. Among them, video recognition [1, 5, 8, 22, 25, 28, 30, 36, 56] is one of the challenging tasks. Similar to image classification, video recognition requires large amounts of annotated data. However, videos have more complex information than images, which needs significant annotation time and resources. To address this challenge, various studies have been conducted to extend semi-supervised learning techniques used in image classification to video recognition [2, 43, 47, 51].

VideoSSL [18] extends the existing semi-supervised image classification methods to the video modality. In addition, MvPL [50] has introduced a multi-modal approach that leverages optical flows and temporal gradients derived from videos. On the other hand, SVFormer [49] recognizes the limitation that image-based augmentation methods, such as mixup, do not perform well in the video domain. To overcome this limitation, SVFormer introduced TubeToken Mixup, which mixes the two different videos at the token level feature. In SSL video recognition, studies considering video and audio modalities are scarce, with AvCLR [3] being a notable exception. However, its augmentation methods focus on individual modalities, overlooking the inter-modal relation between video and audio. Therefore, We introduce a novel approach that employs audio source localization-guided mixup to bridge this gap, considering the interrelation between video and audio.

2.3. Audio Source Localization

Audio source localization is the field of research that combines visual and audio information to identify the source of audio within the scene [34, 35, 45]. Senocak et al. [34] propose the two-stream network architecture that uses attention mechanisms for visual and audio modalities through unsupervised learning. Hu et al. [17] introduce multi-source audio-visual sound localization utilizing contrastive learning and cycle consistency using the synthetic mixture of audio from multiple videos. EZ-VSL [31] proposes multiple instance contrastive learning for alignment between audio-visual modalities and the object-guided localization scheme that utilizes an object localization map generated from a pre-trained visual encoder. FNAC [40] proposes False Negatives Suppression that uses intra-modal similarity to identify potential false negatives and minimize their negative impact, and True Negatives Suppression that encourages more discriminatory sound source localization

by highlighting true negatives using different localization results. We propose an augmentation methodology that utilizes audio source localization to consider the inter-modal relation of video and audio modalities.

3. Methodology

In this section, first, we describe the methodologies primarily used in semi-supervised learning. Then, we introduce the multi-modal video recognition framework that extends to video-audio modalities from the existing video recognition framework. We then introduce our proposed audio source localization-guided mixup methodology.

3.1. Preliminaries

In semi-supervised learning, there are few labeled samples and large-scale unlabeled samples. Let $D_L = \{(x^l, y^l) : l \in [N_L]\}$ as labeled dataset and $D_U = \{(x^u) : u \in [N_U]\}$ as unlabeled dataset where N_L and N_U are numbers of samples in labeled and unlabeled dataset respectively, and in general $N_U \gg N_L$. For the labeled dataset, like the general classification problem, training is conducted through standard cross-entry loss between predicted probabilities and labels like Eq. 1.

$$L_s = \frac{1}{B_l} \sum_i^{B_l} H(y_i^l, p_m(x_i^l)) \quad (1)$$

where B_l is batch size of the labeled data and $p_m(\cdot)$ is denoted predicted probability from the model. In the case of the unlabeled data x^u , consistency regularization is used through data augmentation like weak-augmentation $\alpha_{vid}(\cdot)$ (e.g., random flip or rotation) and strong-augmentation $A_{vid}(\cdot)$ (e.g., RandAugmentation [10]). Throughout these two different augmentation levels, consistency learning is conducted for unlabeled data like Eq. 2.

$$L_u = \frac{1}{B_u} \sum_i^{B_u} H(\hat{p}_m(\alpha_{vid}(x_i^u)), p_m(A_{vid}(x_i^u))) \quad (2)$$

where B_u is the number of unlabeled data in batch and $\hat{p}_m(\cdot)$ can be predicted probability from the Mean Teacher model or model itself by freezing the parameters. And let $\hat{p}_m(\alpha_{vid}(x_i^u))$ as \hat{q}_i^u and $p_m(A_{vid}(x_i^u))$ as Q_i^u . In this case, the predicted probability served as the pseudo label is not reliable, so FixMatch [38] proposes using fixed threshold τ for remaining confidential probability as the pseudo label like Eq. 3.

$$L_u = \frac{1}{B_u} \sum_i^{B_u} \mathbb{1}(\max(\hat{q}_i^u) \geq \tau) H(\hat{q}_i^u, Q_i^u) \quad (3)$$

where $\mathbb{1}(\cdot)$ is the indicator function.

Unlike the fixed threshold approach, which uses a single threshold for all classes, the flexible threshold approach

in FlexMatch [54] sets and updates different thresholds for each class. In Eq.3, τ is replaced with $T = [\tau_1, \dots, \tau_c]$, where c is the number of classes. The flexible threshold for each class is represented by $\tau(\text{argmax}(\hat{q}_i^u))$, where $\text{argmax}(\hat{q}_i^u)$ identifies the class with the highest predicted probability for a given unlabeled sample. The loss function for unlabeled data, as shown in Eq.4, is then defined as:

$$L_u = \frac{1}{B_u} \sum_i^{B_u} \mathbb{1}(\max(\hat{q}_i^u) \geq T(\text{argmax}(\hat{q}_i^u))) H(\hat{q}_i^u, Q_i^u). \quad (4)$$

3.2. Model Pipeline

Our model follows the state-of-the-art semi-supervised learning framework for video action recognition, SVFormer [49]. This framework utilizes the consistency loss based on FixMatch, along with augmentation methods for video modality, namely TubeToken Mix (TTMix) and Temporal Warping Augmentation (TWAug).

Let two unlabeled video clips as $v_a^u, v_b^u \in \mathbb{R}^{H \times W \times C \times T}$ where (H, W) is the resolution of the image frame, C is the number of the channels and T is the number of the frames in the video clip, and let two embedded vectors $Emb_{vid}(v_a^u), Emb_{vid}(v_b^u) \in \mathbb{R}^{N \times (P^2 \cdot C) \times T}$ where P is the non-overlapping patch size and $N = HW/P^2$ is the number of the embedding patches. For the mixing of two embedded video clips, token-level mask $\mathbf{M} \in \{0, 1\}^{(P^2 \cdot C) \times T}$ is utilized as Eq. 5.

$$e_{mix}^u = Emb_{vid}(A_{vid}(v_a^u)) \odot \mathbf{M} + Emb_{vid}(A_{vid}(v_b^u)) \odot (1 - \mathbf{M}) \quad (5)$$

where \odot is element-wise multiplication.

At this point, SVFormer utilizes tube-style masking, which shares the same mask pattern through all the frames and has consistency in the temporal axis, rather than frame token masking and random token masking. In the case of TWAug, it is utilized for stretching one frame to various temporal lengths. For example, given the number of T frames, they select a few frames and pad with chosen frames at the other frame positions that are not selected. By this TWAug, they argue that the model can learn temporal dynamics flexibly.

Although most commonly encountered videos contain sequences of frames and corresponding audio information, many studies pay less attention to audio information. Inspired by this respect, we expand the SVFormer framework to video-audio modalities.

Let unlabeled audio log mel-filterbank feature data as $a_a^u, a_b^u \in \mathbb{R}^{M \times L}$ from corresponding video clips v_a^u, v_b^u , respectively, where L is time-step and M is range of the mel-frequency. For the augmentation, we use SpecAugment [32] as strong-augmentation $A_{aud}(\cdot)$. Through the Eq. 6, mixed audio is conducted.

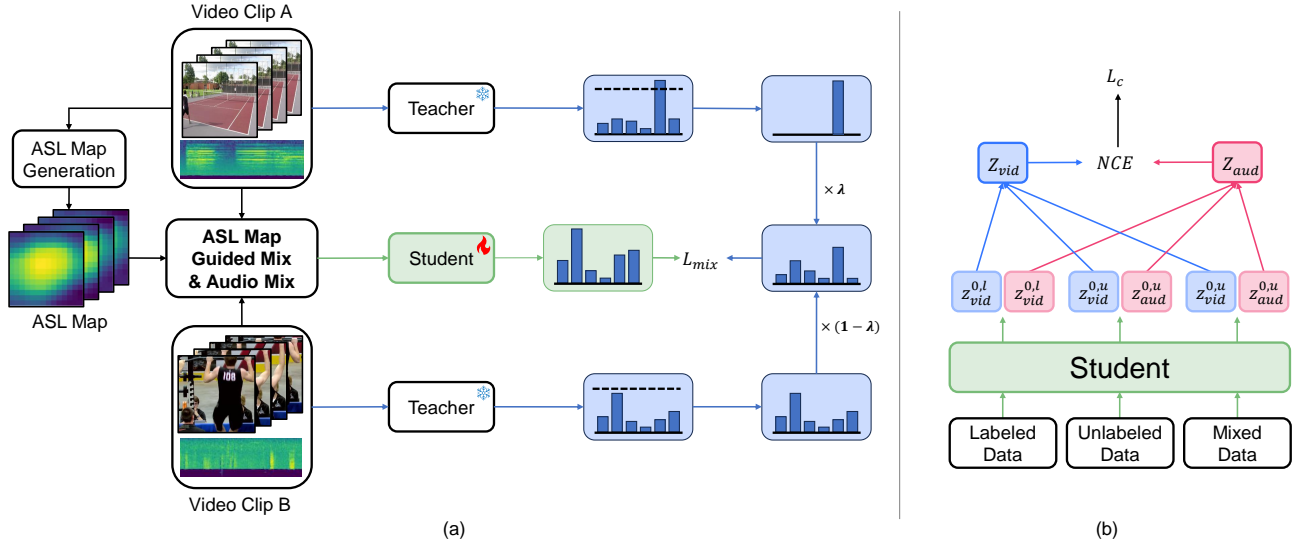


Figure 1. **Overview of audio source localization-guided mixup framework.** The framework performs audio source localization-guided mixup on video clips A and B. A localization map from video A is used to create a mask that highlights semantically important regions, considering the interrelation between video and audio. Log mel-filterbank coefficients of audios A and B are then interpolated, and the mixed video and audio are used for prediction.

$$a_{mix}^u = \lambda \cdot A_{aud}(a_a^u) + (1 - \lambda) \cdot A_{aud}(a_b^u) \quad (6)$$

where λ is the hyper-parameter that follows the beta-distribution used for the mixup.

The following discussion focuses on the process of learning utilizing video and audio data. Initially, a [cls] token is concatenated to the previously obtained embedding, and this combined embedding is then fed into the video encoder E_{vid} . As a result, the output z_{vid} is calculated. Similarly, for audio, after embedding the audio, it is input into the audio encoder E_{aud} , resulting in the output z_{aud} . This calculation is applied in the same way to video clips v_a^u, v_b^u and their corresponding audio a_a^u, a_b^u as well as to the mixed video and audio obtained from Eq. 5 and 6. This process can be verified through the following equations.

$$z_{vid} = E_{vid}([\text{CLS}_{vid}, e_{mix}^u]) \quad (7)$$

$$z_{aud} = E_{aud}([\text{CLS}_{aud}, Emb_{aud}(a_{mix}^u)]) \quad (8)$$

$$\hat{y} = \text{FUSION}(z_{vid}^0, z_{aud}^0) \quad (9)$$

where z_{vid}^0, z_{aud}^0 means the first token of z_{vid}, z_{aud} , and $\text{FUSION}(\cdot)$ means a fusion model consisting of transformer encoder layers.

In the same manner, by forwarding $\alpha_{vid}(v_a^u), \alpha_{vid}(v_b^u)$ and a_a^u, a_b^u into the teacher model, we can calculate \hat{y}_a and \hat{y}_b . Then, using the calculated \hat{y}_a and \hat{y}_b along with λ from Eq. 6, we compute the pseudo label \bar{y}_{mix} . This is used to optimize the model through the consistency loss as described in Eq. 10.

$$L_{mix} = \frac{1}{B_u} \sum \mathbb{1}(\max(\bar{y}_{mix}) \geq \tau) (\bar{y}_{mix} - \hat{y}_{mix})^2 \quad (10)$$

3.3. Audio Source Localization-guided Mixup

However, we observe that video and audio are augmented only within their respective modalities in the framework in Section 3.2. This approach does not consider the interrelation between the visual and audio information, even though they share the same video clip. Therefore, we propose the novel audio source localization-guided mixup. If the mask is generated through sampling from the audio source localization map and provided as the guide, the relationship between video and audio can be considered when performing the mixup.

We introduce the audio source localization model that is composed of a visual encoder $E_{vid}^{as}(\cdot)$ and an audio encoder $E_{aud}^{as}(\cdot)$. For v^u and a^u sharing a video clip, $A_{vid}(v^u)$ is feed into $E_{vid}^{as}(\cdot)$, and $A_{aud}(a^u)$ is similarly feed into $E_{aud}^{as}(\cdot)$.

As a result, the visual feature f_{vid} and the audio feature f_{aud} are calculated. To compute their respective attention maps f_{vid}^{attn} and f_{aud}^{attn} , we perform matrix multiplication on the transposed features as shown in Eq. 11. Subsequently, we generate the final audio source localization map MAP using dot product operations as outlined in Eq. 12.

$$f_{vid}^{attn} = (f_{vid})(f_{vid})^T, \quad f_{aud}^{attn} = (f_{aud})(f_{aud})^T \quad (11)$$

$$\text{MAP} = (f_{vid}^{attn})(f_{aud}^{attn})^T \quad (12)$$

Building upon this, we can construct the novel mask M_{as} to replace the token-level mask M utilized in Eq. 5. We interpolate MAP to align with the dimensions of $Emb_{vid}(v^u)$, resulting in an interpolated map denoted as MAP' . By nor-

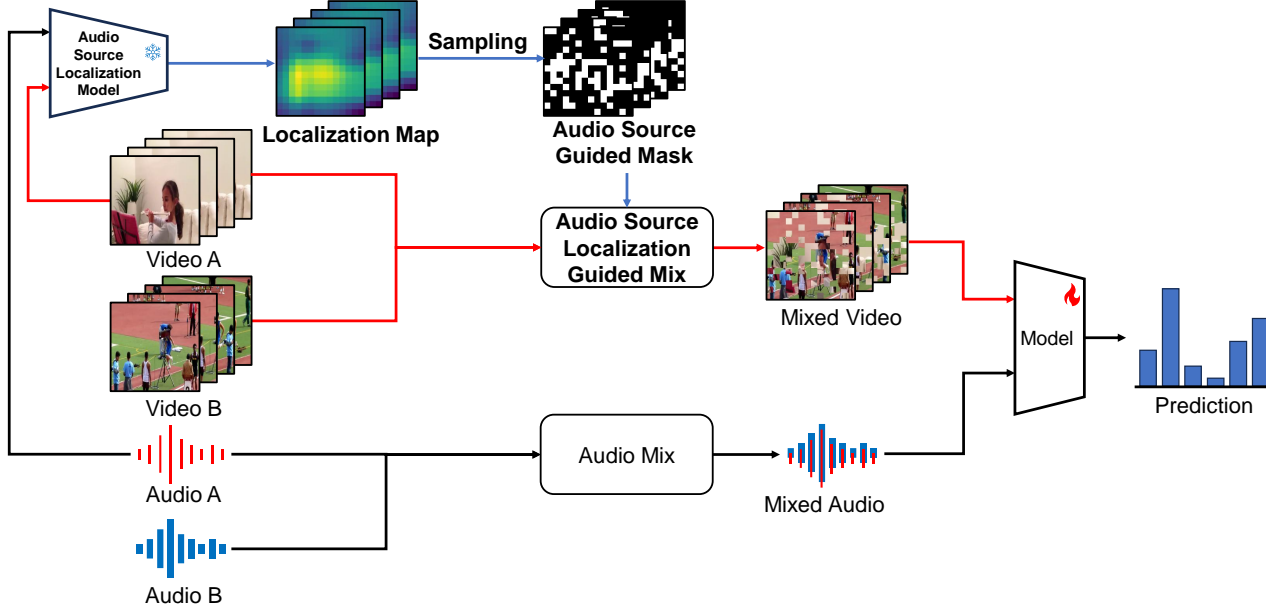


Figure 2. **Overview of our audio source localization-guided mixup framework.** The framework performs the audio source localization-guided mixup on video clips A and B. For generating the audio source localization map, video clip A is utilized. The video and audio from clip A are processed through an audio source localization model to produce the localization maps. This generated map is then used as the weight for performing multinomial sampling without replacement, creating an audio source localization-guided mask. Considering the audio information, this mask guides semantically important regions in video A. Consequently, our proposed audio source localization-guided mixup allows consideration of the interrelation between video and audio modalities sharing the same video clip. For audio A and B, log mel-filterbank coefficients are transformed and interpolated at the pixel level. The resulting mixed video and audio are then used as input for prediction.

malizing MAP' with min-max normalization, we provide a basis for probabilistically selecting locations likely to contain the audio source. Employing multinomial distribution probabilities, we sample without replacement using MAP' as weights. This process generates the new mask M_{as} , allowing us to retain $(\lambda \cdot N)$ tokens of $\text{Emb}_{vid}(v^u)$ for use. We visualize the differences between our proposed audio source localization-guided mask and the TubeToken mask in Fig. 3.

3.4. Visual-Audio Contrastive Learning

To align visual and audio information, we employ a visual-audio contrastive learning loss. This approach utilizes the embeddings z_{vid}^0 and z_{aud}^0 , obtained from Eq. 7 and 8, respectively. Considering labeled, unlabeled, and mixed data, we define the video embeddings matrix $Z_{vid}^l, Z_{vid}^u, Z_{vid}^m$ in Eq. 13, where $i \in [B_l]$ and $j \in [B_u]$. A similar definition applies to the audio embeddings matrix Z_{aud} .

First, we perform L2 normalization on Z_{vid} and Z_{aud} . The similarity between video and audio is then computed using matrix multiplication as shown in Eq. 15, resulting in the visual-audio similarity matrix S .

$$Z_{vid} = [z_{vid}^{l_{0,1}}, \dots, z_{vid}^{l_{0,i}}; z_{vid}^{u_{0,1}}, \dots, z_{vid}^{u_{0,j}}; z_{vid}^{m_{0,1}}, \dots, z_{vid}^{m_{0,j}}] \quad (13)$$

$$Z'_{vid} = \frac{Z_{vid}}{\|Z_{vid}\|_2}, \quad Z'_{aud} = \frac{Z_{aud}}{\|Z_{aud}\|_2} \quad (14)$$

$$S = \frac{1}{0.05} \cdot Z'_{aud}(Z'_{vid})^T \quad (15)$$

Subsequently, we compute the visual-audio contrastive loss L_c using the noise-contrastive estimation loss applied to S .

$$\text{NCE}_1 = -\frac{1}{K} \sum_{i=1}^K \log \left(\frac{e^{S_{ii}}}{\sum_{j=1}^K e^{S_{ij}}} \right), \quad (16)$$

$$\text{NCE}_2 = -\frac{1}{K} \sum_{i=1}^K \log \left(\frac{e^{S_{ii}}}{\sum_{j=1}^K e^{S_{ji}}} \right) \quad (17)$$

$$L_c = \frac{\text{NCE}_1 + \text{NCE}_2}{2} \quad (18)$$

Here, K denotes the number of elements in Z_{vid} and Z_{aud} .

3.5. Training Objective

Our proposed model requires four main types of loss functions for training. These include the supervised learning loss (Eq. 1), the consistency regularization loss for un-

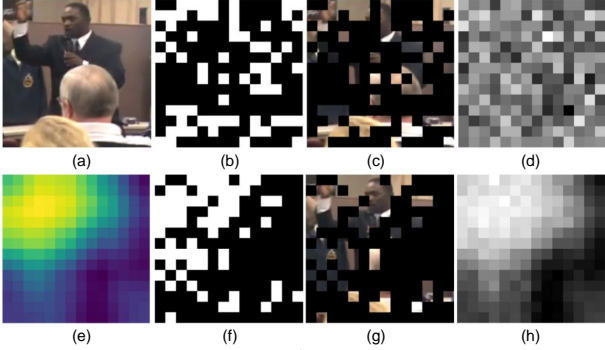


Figure 3. **Visualization of the TubeToken mask and our proposed Audio Source Localization-guided Mask.** When an original image (a) is given, the TubeToken masking creates a random pattern mask (b), resulting in a masked image (c) for SVFormer input. Sampling this mask 255 times yields an average TubeToken Mask (d). Our method uses an audio source localization-guided mask. Starting with the original image (a), a localization map (e) is generated and used as a weight for sampling, creating the guided mask (f). Applying this mask to the original image results in (g). Sampling this mask 255 times produces (h), highlighting audio source areas and allowing for visual-audio modality mixup.

labeled data (Eq. 4), and the contrastive loss for aligning visual and audio modalities (Eq. 18). Additionally, we utilize a consistency regularization loss for a mixture of unlabeled data, guided by audio source localization mixup (Eq. 10). The total loss used for training is formulated as follows:

$$L_{total} = L_s + \gamma_1 \cdot L_u + \gamma_2 \cdot L_{mix} + \gamma_3 \cdot L_c \quad (19)$$

where γ_1 , γ_2 , and γ_3 are the hyper-parameters for balancing the each loss.

4. Experiment

In this section, we first explain the experimental setting. Next, we analyze the experimental results conducted with different numbers of labeled data on different datasets and discuss ablation studies.

4.1. Experimental Setting

Datasets We conduct experiments using three datasets: UCF-51 [39], Kinetics-400 [19], and VGGSound [7]. UCF-51 is a refined subset of the UCF-101 dataset, comprising 51 classes, including audio, consisting of 4.9K training and 1.4K test samples. Kinetics-400 covers 400 categories, each with approximately 10-second-long videos, amounting to 240K training and 20K validation samples. For this dataset, samples without audio are filtered out. VGGSound is composed of around 200K videos, each about 10 seconds in length, and provides annotations for 309 categories. After excluding unavailable videos, we have 183,730 training samples and 15,446 test samples. Before the experiments, the UCF-51, Kinetics-400, and VGGSound datasets are split to ensure each class contains 1 and 5 labeled data sam-

ples, respectively. Using one labeled data sample per class is a more extremely challenging experimental condition, which has also been used in semi-supervised image classification studies [29, 46]. Additionally, using five labeled data samples per class is similar to other studies [49–51] that take a 1% labeled samples setting, which uniformly uses only six labeled samples per class, despite the dataset being imbalanced.

Baselines We use the prior studies LTG [48], SVFormer [49], and the state-of-the-art audio-visual semi-supervised action recognition, AvCLR [3], as our baselines. However, in the case of AvCLR, the implementation codes are not public, so we report the results of their study. Additionally, we employ a model that modifies the fixed threshold used in the original SVFormer to a flexible threshold. The majority of the hyper-parameters are set up identically to those in SVFormer.

Evaluation We utilize top-1 accuracy as the metric. Given the potential unfairness of comparing CNN-based methods directly with Transformer-based methods, it is worth noting that our comparison is made directly with SVFormer, the state-of-the-art semi-supervised video action recognition model, instead of directly comparing with CNN-based.

4.2. Implementation Details

For training, we follow the SVFormer settings. All experiments are conducted with $2 \times$ A100 80GB GPUs. We utilize the FNAC [40] as the audio source localization model. FNAC is a two-stream network comprising two ResNet-18 models, serving as the visual and audio encoders, respectively. During the training phase, we use a version of FNAC pre-trained on the Flickr-1K dataset [33] without object-guided localization. This model is kept frozen and is not further trained during our training phase. We set the ratio between labeled and unlabeled samples as 1:5 in the mini-batch following SVFormer’s setting. Also, we use an SGD optimizer for training, with a momentum of 0.9 and a weight decay of 0.001. The exponential moving average from the student model serves as the teacher model in both SVFormer and ours.

The values of γ_1 and γ_2 are set to 2, while for γ_3 , we select the optimal value from $\{0.1, 0.2, 0.3\}$. Additionally, for the masking ratio λ , we sample from the beta distribution $\text{Beta}(\alpha_1, \alpha_2)$, setting α_1 to 5 and α_2 to 10. This is because, guided by audio source localization, it is acceptable to take a smaller ratio of the video for creating the localization map due to the selection of significant regions. During the testing phase, the entire video is uniformly divided into five parts, and we perform cropping three times to cover most areas of the video clip, each with a size of 224×224 . For the final testing prediction, we averaged a total of 15 predictions obtained by performing the aforementioned three crops five times per video clip.

| Model | Backbone | Input | Epoch | Threshold Type | Mask Type | UCF-51 | | Kinetic400 | | VGGSound | |
|---------------|-----------|-------|-------|----------------|------------|--------------|--------------|--------------|--------------|--------------|--------------|
| | | | | | | 51 | 255 | 400 | 2000 | 309 | 1545 |
| TCL [37] | TSM-Res18 | V | 400 | Fix | - | 9.16 | 25.93 | 1.18 | 2.26 | 0.43 | 0.66 |
| LTG [48] | 3D-Res18 | V, G | 180 | Fix | - | 16.51 | 49.74 | 0.46 | 3.39 | 0.37 | 0.45 |
| AvCLR [3] | 3D-Res18 | V, A | 800 | Fix | - | - | 50.1 | - | - | - | - |
| SVFormer [49] | ViT-B | V | 50 | Fix | TubeToken | 60.75 | 87.71 | 16.01 | 46.93 | 14.87 | 37.70 |
| | ViT-B | V | 50 | Flex | TubeToken | 63.58 | 86.63 | 16.69 | 47.62 | 15.98 | 36.72 |
| Ours | ViT-B | V, A | 50 | Flex | ASL-Guided | 72.58 | 89.09 | 19.12 | 48.64 | 17.49 | 38.00 |

Table 1. **Top-1 accuracy comparisons with state-of-the-art methods on UCF-51, Kinetics-400, and VGGSound.** Note that TCL, LTG, and AvCLR are CNN-based, while SVFormer and ours use Transformer architectures. ‘V’, ‘A’, and ‘G’ represent video, audio, and temporal gradient modalities. ‘Fix’ refers to the fixed threshold from FixMatch [38], and ‘Flex’ to the flexible threshold from FlexMatch [54]. ‘TubeToken’ is SVFormer’s mask strategy, and ‘ASL-Guided’ is our proposed Audio Source Localization-Guided method. The numbers below each dataset show the amount of labeled data used in training.

| Input Type | Mask Type | Contrastive | Trainable Params. | GFLOPs | Accuracy |
|------------|-----------|-------------|-------------------|---------|--------------|
| V | TubeToken | | 121M | 761.144 | 63.58 |
| V,A | TubeToken | | 254M | 805.167 | 66.72 |
| V,A | TubeToken | ✓ | 254M | 805.167 | 68.52 |
| V,A | Proposed | | 254M | 820.998 | 71.55 |
| V,A | Proposed | ✓ | 254M | 820.998 | 72.58 |

Table 2. **Ablation study about using audio source localization-guided mask and contrastive learning.** This experiment is conducted on the UCF-51 dataset using one labeled sample per class. It aims to understand the effectiveness of our proposed ASL mask and audio-visual contrastive learning.

4.3. Main Results

The main experimental results on UCF-51, Kinetics-400, and VGGSound datasets can be found in Table 1. Compared to previous methods, our proposed method demonstrates superior performance. Specifically, on the UCF-51 dataset, using only one labeled sample per class, we achieve an absolute performance improvement of 9.00% accuracy and also a relative accuracy improvement of 14.1% over the SVFormer, which only uses video modality with flexible thresholding. Moreover, on Kinetics-400, our model outperforms SVFormer by 2.43% and 15.56%, and on VGGSound, we achieve 1.51% and 9.45% higher performances in absolute and relative accuracy improvement, respectively. Even though the gains become smaller when considering performance with five samples per class, which is easier, our approach still outperforms baselines and improves performance. These results demonstrate the effectiveness of our proposed audio source localization-guided mixup method in considering the intermodal relation between video and audio modalities.

Our method, which leverages the visual-audio modality in a semi-supervised learning approach and considers the relationship between video and audio, outperforms the state-of-the-art CNN-based AvCLR by 38.99% on UCF-51. However, due to the unavailability of AvCLR’s code, we are limited to comparing it against its published results only. This limitation may raise concerns about whether the per-

formance difference is solely due to the backbone architecture (CNN vs. Transformer). To address these concerns and demonstrate that the effectiveness of our method goes beyond architectural differences, we provide additional experiments in Section 4.4.

4.4. Ablation Studies

To understand the impacts of the proposed methods, we conduct the ablation studies on UCF-51.

Analysis of Mask Type and Contrastive Learning To evaluate the effectiveness of our proposed methodologies, we conduct an ablation study focusing on the audio source localization-guided mask (ASL mask) and visual-audio contrastive learning, and the result is in Table 2. Initially, we observe that integrating both video and audio modalities enhances performance by a margin of 3.14%. Furthermore, when applying visual-audio contrastive learning, we note an additional performance increase of 1.80%. Even though the integration of an additional audio encoder and fusion module increases the number of trainable parameters to utilize the audio modality, it significantly boosts overall performance. The empirical evidence supports that the utilization of audio modality contributes positively.

A noteworthy outcome of our study is the performance improvement of 4.83% achieved by employing the ASL mask over the TubeToken mask. This improvement becomes even more significant when the ASL mask is combined with contrastive learning, achieving an accuracy of 72.58%. These findings demonstrate the effectiveness of our audio source localization-guided mixup in considering the inter-modal relation between video and audio modalities. At the same time, visual-audio contrastive learning contributes to further performance enhancements.

The additional computations obtained by adding audio modality and applying the proposed mask strategy are small compared to existing video computations in a single training iteration. Considering the substantial performance gains, the additional computational load is manageable.

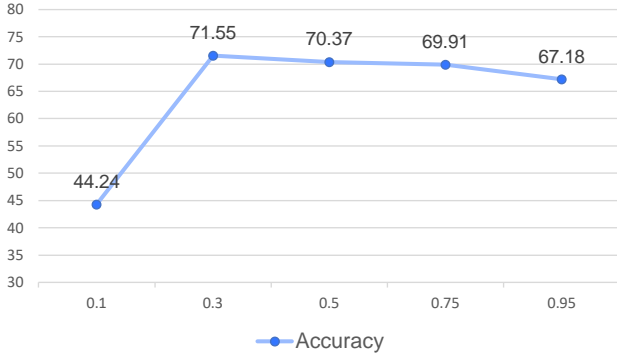


Figure 4. **Impact of threshold (τ).** This figure presents the results of experiments conducted to explore the performance impact of the hyper-parameter τ . It specifically focuses on the changes in performance with varying thresholds of τ during training with only one labeled sample in the UCF-51 dataset.

Threshold for Pseudo Label We conduct an ablation study to assess the impact of the threshold τ for generating pseudo labels in our proposed audio source localization guided-mixup method. In this study, the predicted probability calculated by the teacher model is used as a pseudo label, and we explore how different τ values affect this process.

We observed that a lower threshold of 0.1 generally results in most predicted probabilities being used as pseudo labels. However, this can lead to performance degradation due to the accumulation of bias from low-confidence pseudo-labels.

Moreover, ours of the flexible thresholding method proposed in FlexMatch [54] allows us to maintain superior performance compared to SVFormer, which also incorporates audio modality, even as τ increases. Among various τ values, we identified 0.3 as the optimal value and set it for our main experiments and other ablation studies. The performance variations according to different τ values can be seen in Fig. 4.

Mask Sampling per Varying Frames Inspired by the applications of tube-shaped masks in the video domain [44, 49], which utilize consistent tokens across time to prevent information leakage from adjacent frames, we conduct an ablation study on the creation of audio source localization masks. This study involves averaging maps generated from adjacent frames and using these averages for sampling to create masks. Our experiments are designed to test averages over 1, 2, 4, 8 frames. The results of this experiment can be seen in Fig. 5.

From our findings, we observe that contrary to the TubeToken mask approach, generating masks based on each individual frame achieves the best performance for our proposed audio source localization-guided masks. This can be attributed to the fact that while audio source localization

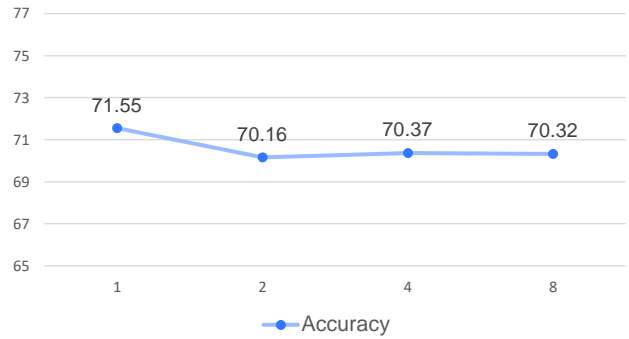


Figure 5. **Ablation study on the effect of varying frame counts (1, 2, 4, and 8 frames) on the audio source localization map.** This study evaluates the impact of averaging the localization maps over different numbers of frames before using them in the sampling process.

maps are generated for each frame based on visual and audio information, the visual information varies from frame to frame. Therefore, when using the average of audio source localization maps generated from different frames, it can prevent information leakage from adjacent frames during token-level mixup, similar to the TubeToken approach. This method might be effective for static videos with minimal audio source location changes. However, for videos with rapid changes, this averaging approach uses a mean of different audio source locations, which may not accurately represent the true location in dynamic scenes. Consequently, this can lead to significant information loss and, ultimately, a decrease in performance.

5. Conclusion

This paper introduces a transformer-based semi-supervised multimodal video action recognition approach, expanding the previous visual framework to include visual-audio information from video clips. To address the limitations of existing augmentation methods that only consider individual modalities, we propose the audio source localization-guided mixup, which considers the interrelation between visual and audio information. Our method demonstrates superior performance over state-of-the-art methods on the UCF-51, Kinetics-400, and VGGSound datasets. While our approach relies on the audio source localization method, we anticipate that our performance will further improve as audio source localization techniques advance. Incorporating audio modalities into SVFormer [49] requires an additional encoder and fusion module, which increases computational costs. Nevertheless, our method enhances performance and explores the relationships between visual and audio modalities, demonstrating that a comprehensive understanding of these relationships can significantly boost performance.

References

- [1] Anurag Arnab, Mostafa Dehghani, Georg Heigold, Chen Sun, Mario Lučić, and Cordelia Schmid. Vivit: A video vision transformer. In *Proceedings of the IEEE/CVF international conference on computer vision*, pages 6836–6846, 2021. [2](#)
- [2] Maregu Assefa, Wei Jiang, Kumie Gedamu, Getinet Yilma, Deepak Adhikari, Melese Ayalew, Abegaz Mohammed, and Aiman Erbad. Actor-aware self-supervised learning for semi-supervised video representation learning. *IEEE Transactions on Circuits and Systems for Video Technology*, 2023. [2](#)
- [3] Maregu Assefa, Wei Jiang, Jinyu Zhan, Kumie Gedamu, Getinet Yilma, Melese Ayalew, and Deepak Adhikari. Audio-visual contrastive and consistency learning for semi-supervised action recognition. *IEEE Transactions on Multimedia*, 2023. [1](#), [2](#), [6](#), [7](#)
- [4] David Berthelot, Nicholas Carlini, Ian Goodfellow, Nicolas Papernot, Avital Oliver, and Colin A Raffel. Mixmatch: A holistic approach to semi-supervised learning. *Advances in neural information processing systems*, 32, 2019. [2](#)
- [5] Shweta Bhardwaj, Mukundhan Srinivasan, and Mitesh M Khapra. Efficient video classification using fewer frames. In *Proceedings of the IEEE/CVF Conference on Computer Vision and Pattern Recognition*, pages 354–363, 2019. [2](#)
- [6] Baixu Chen, Janguang Jiang, Ximei Wang, Pengfei Wan, Jianmin Wang, and Mingsheng Long. Debaised self-training for semi-supervised learning. *Advances in Neural Information Processing Systems*, 35:32424–32437, 2022. [1](#)
- [7] Honglie Chen, Weidi Xie, Andrea Vedaldi, and Andrew Zisserman. Vggsound: A large-scale audio-visual dataset. In *ICASSP 2020-2020 IEEE International Conference on Acoustics, Speech and Signal Processing (ICASSP)*, pages 721–725. IEEE, 2020. [6](#)
- [8] Jiawei Chen and Chiu Man Ho. Mm-vit: Multi-modal video transformer for compressed video action recognition. In *Proceedings of the IEEE/CVF winter conference on applications of computer vision*, pages 1910–1921, 2022. [1](#), [2](#)
- [9] Yuhao Chen, Xin Tan, Borui Zhao, Zhaowei Chen, Renjie Song, Jiajun Liang, and Xuequan Lu. Boosting semi-supervised learning by exploiting all unlabeled data. In *Proceedings of the IEEE/CVF Conference on Computer Vision and Pattern Recognition*, pages 7548–7557, 2023. [1](#)
- [10] Ekin D Cubuk, Barret Zoph, Jonathon Shlens, and Quoc V Le. Randaugment: Practical automated data augmentation with a reduced search space. In *Proceedings of the IEEE/CVF conference on computer vision and pattern recognition workshops*, pages 702–703, 2020. [1](#), [3](#)
- [11] Ishan Rajendrakumar Dave, Mamshad Nayeem Rizve, Chen Chen, and Mubarak Shah. Timebalance: Temporally-invariant and temporally-distinctive video representations for semi-supervised action recognition. In *Proceedings of the IEEE/CVF Conference on Computer Vision and Pattern Recognition*, pages 2341–2352, 2023. [1](#), [2](#)
- [12] W Dong-DongChen and ZH WeiGao. Tri-net for semi-supervised deep learning. In *Proceedings of twenty-seventh international joint conference on artificial intelligence*, pages 2014–2020, 2018. [2](#)
- [13] Alexey Dosovitskiy, Lucas Beyer, Alexander Kolesnikov, Dirk Weissenborn, Xiaohua Zhai, Thomas Unterthiner, Mostafa Dehghani, Matthias Minderer, Georg Heigold, Sylvain Gelly, et al. An image is worth 16x16 words: Transformers for image recognition at scale. *arXiv preprint arXiv:2010.11929*, 2020. [2](#)
- [14] Shreyank N Gowda, Marcus Rohrbach, Frank Keller, and Laura Sevilla-Lara. Learn2augment: learning to composite videos for data augmentation in action recognition. In *European conference on computer vision*, pages 242–259. Springer, 2022. [1](#)
- [15] Kaiming He, Xiangyu Zhang, Shaoqing Ren, and Jian Sun. Deep residual learning for image recognition. In *Proceedings of the IEEE conference on computer vision and pattern recognition*, pages 770–778, 2016. [2](#)
- [16] Andrew G Howard, Menglong Zhu, Bo Chen, Dmitry Kalenichenko, Weijun Wang, Tobias Weyand, Marco Andreetto, and Hartwig Adam. Mobilenets: Efficient convolutional neural networks for mobile vision applications. *arXiv preprint arXiv:1704.04861*, 2017. [2](#)
- [17] Xixi Hu, Ziyang Chen, and Andrew Owens. Mix and localize: Localizing sound sources in mixtures. In *Proceedings of the IEEE/CVF Conference on Computer Vision and Pattern Recognition*, pages 10483–10492, 2022. [2](#)
- [18] Longlong Jing, Toufiq Parag, Zhe Wu, Yingli Tian, and Hongcheng Wang. Videoss1: Semi-supervised learning for video classification. In *Proceedings of the IEEE/CVF Winter Conference on Applications of Computer Vision*, pages 1110–1119, 2021. [1](#), [2](#)
- [19] Will Kay, Joao Carreira, Karen Simonyan, Brian Zhang, Chloe Hillier, Sudheendra Vijayanarasimhan, Fabio Viola, Tim Green, Trevor Back, Paul Natsev, et al. The kinetics human action video dataset. *arXiv preprint arXiv:1705.06950*, 2017. [6](#)
- [20] Alex Krizhevsky, Ilya Sutskever, and Geoffrey E Hinton. Imagenet classification with deep convolutional neural networks. *Advances in neural information processing systems*, 25, 2012. [2](#)
- [21] Samuli Laine and Timo Aila. Temporal ensembling for semi-supervised learning. *arXiv preprint arXiv:1610.02242*, 2016. [2](#)
- [22] Sumin Lee, Sangmin Woo, Yeonju Park, Muhammad Adi Nugroho, and Changick Kim. Modality mixer for multi-modal action recognition. In *Proceedings of the IEEE/CVF Winter Conference on Applications of Computer Vision*, pages 3298–3307, 2023. [1](#), [2](#)
- [23] KunChang Li, Yanan He, Yi Wang, Yizhuo Li, Wenhai Wang, Ping Luo, Yali Wang, Limin Wang, and Yu Qiao. Videochat: Chat-centric video understanding. *arXiv preprint arXiv:2305.06355*, 2023. [1](#), [2](#)
- [24] Kunchang Li, Yali Wang, Yanan He, Yizhuo Li, Yi Wang, Limin Wang, and Yu Qiao. Uniformerv2: Unlocking the potential of image vits for video understanding. In *Proceedings of the IEEE/CVF International Conference on Computer Vision*, pages 1632–1643, 2023. [1](#), [2](#)

- [25] Yanghao Li, Chao-Yuan Wu, Haoqi Fan, Karttikeya Mangalam, Bo Xiong, Jitendra Malik, and Christoph Feichtenhofer. Mvity2: Improved multiscale vision transformers for classification and detection. In *Proceedings of the IEEE/CVF Conference on Computer Vision and Pattern Recognition*, pages 4804–4814, 2022. 2
- [26] Yang Liu, Keze Wang, Lingbo Liu, Haoyuan Lan, and Liang Lin. Tcgl: Temporal contrastive graph for self-supervised video representation learning. *IEEE Transactions on Image Processing*, 31:1978–1993, 2022. 1, 2
- [27] Ze Liu, Yutong Lin, Yue Cao, Han Hu, Yixuan Wei, Zheng Zhang, Stephen Lin, and Baining Guo. Swin transformer: Hierarchical vision transformer using shifted windows. In *Proceedings of the IEEE/CVF international conference on computer vision*, pages 10012–10022, 2021. 2
- [28] Ze Liu, Jia Ning, Yue Cao, Yixuan Wei, Zheng Zhang, Stephen Lin, and Han Hu. Video swin transformer. In *Proceedings of the IEEE/CVF conference on computer vision and pattern recognition*, pages 3202–3211, 2022. 2
- [29] Thomas Lucas, Philippe Weinzaepfel, and Gregory Rogez. Barely-supervised learning: Semi-supervised learning with very few labeled images. In *Proceedings of the AAAI Conference on Artificial Intelligence*, volume 36, pages 1881–1889, 2022. 6
- [30] Feng Mao, Xiang Wu, Hui Xue, and Rong Zhang. Hierarchical video frame sequence representation with deep convolutional graph network. In *Proceedings of the European conference on computer vision (ECCV) workshops*, pages 0–0, 2018. 2
- [31] Shentong Mo and Pedro Morgado. Localizing visual sounds the easy way. In *European Conference on Computer Vision*, pages 218–234. Springer, 2022. 2
- [32] Daniel S Park, William Chan, Yu Zhang, Chung-Cheng Chiu, Barret Zoph, Ekin D Cubuk, and Quoc V Le. SpecAugment: A simple data augmentation method for automatic speech recognition. *arXiv preprint arXiv:1904.08779*, 2019. 3
- [33] Bryan A Plummer, Liwei Wang, Chris M Cervantes, Juan C Caicedo, Julia Hockenmaier, and Svetlana Lazebnik. Flickr30k entities: Collecting region-to-phrase correspondences for richer image-to-sentence models. In *Proceedings of the IEEE international conference on computer vision*, pages 2641–2649, 2015. 6
- [34] Arda Senocak, Tae-Hyun Oh, Junsik Kim, Ming-Hsuan Yang, and In So Kweon. Learning to localize sound source in visual scenes. In *Proceedings of the IEEE Conference on Computer Vision and Pattern Recognition*, pages 4358–4366, 2018. 2
- [35] Arda Senocak, Hyeonggon Ryu, Junsik Kim, Tae-Hyun Oh, Hanspeter Pfister, and Joon Son Chung. Sound source localization is all about cross-modal alignment. In *Proceedings of the IEEE/CVF International Conference on Computer Vision*, pages 7777–7787, 2023. 2
- [36] Muhammad Bilal Shaikh, Douglas Chai, Syed Mohammed Shamsul Islam, and Naveed Akhtar. Maivar-t: Multimodal audio-image and video action recognizer using transformers. In *2023 11th European Workshop on Visual Information Processing (EUVIP)*, pages 1–6. IEEE, 2023. 1, 2
- [37] Ankit Singh, Omprakash Chakraborty, Ashutosh Varshney, Rameswar Panda, Rogerio Feris, Kate Saenko, and Abir Das. Semi-supervised action recognition with temporal contrastive learning. In *Proceedings of the IEEE/CVF Conference on Computer Vision and Pattern Recognition*, pages 10389–10399, 2021. 7
- [38] Kihyuk Sohn, David Berthelot, Nicholas Carlini, Zizhao Zhang, Han Zhang, Colin A Raffel, Ekin Dogus Cubuk, Alexey Kurakin, and Chun-Liang Li. Fixmatch: Simplifying semi-supervised learning with consistency and confidence. *Advances in neural information processing systems*, 33:596–608, 2020. 1, 2, 3, 7
- [39] Khurram Soomro, Amir Roshan Zamir, and Mubarak Shah. Ucf101: A dataset of 101 human actions classes from videos in the wild. *arXiv preprint arXiv:1212.0402*, 2012. 6
- [40] Weixuan Sun, Jiayi Zhang, Jianyuan Wang, Zheyuan Liu, Yiran Zhong, Tianpeng Feng, Yandong Guo, Yanhao Zhang, and Nick Barnes. Learning audio-visual source localization via false negative aware contrastive learning. In *Proceedings of the IEEE/CVF Conference on Computer Vision and Pattern Recognition*, pages 6420–6429, 2023. 2, 6
- [41] Christian Szegedy, Wei Liu, Yangqing Jia, Pierre Sermanet, Scott Reed, Dragomir Anguelov, Dumitru Erhan, Vincent Vanhoucke, and Andrew Rabinovich. Going deeper with convolutions. In *Proceedings of the IEEE conference on computer vision and pattern recognition*, pages 1–9, 2015. 2
- [42] Antti Tarvainen and Harri Valpola. Mean teachers are better role models: Weight-averaged consistency targets improve semi-supervised deep learning results. *Advances in neural information processing systems*, 30, 2017. 2
- [43] Anyang Tong, Chao Tang, and Wenjian Wang. Semi-supervised action recognition from temporal augmentation using curriculum learning. *IEEE Transactions on Circuits and Systems for Video Technology*, 33(3):1305–1319, 2022. 1, 2
- [44] Zhan Tong, Yibing Song, Jue Wang, and Limin Wang. Videomae: Masked autoencoders are data-efficient learners for self-supervised video pre-training. *Advances in neural information processing systems*, 35:10078–10093, 2022. 1, 2, 8
- [45] Sung Jin Um, Dongjin Kim, and Jung Uk Kim. Audio-visual spatial integration and recursive attention for robust sound source localization. In *Proceedings of the 31st ACM International Conference on Multimedia*, pages 3507–3516, 2023. 2
- [46] Yidong Wang, Hao Chen, Qiang Heng, Wenxin Hou, Yue Fan, Zhen Wu, Jindong Wang, Marios Savvides, Takahiro Shinozaki, Bhiksha Raj, et al. Freematch: Self-adaptive thresholding for semi-supervised learning. *arXiv preprint arXiv:2205.07246*, 2022. 1, 2, 6
- [47] Jianlong Wu, Wei Sun, Tian Gan, Ning Ding, Feijun Jiang, Jialie Shen, and Liqiang Nie. Neighbor-guided consistent and contrastive learning for semi-supervised action recognition. *IEEE Transactions on Image Processing*, 2023. 2
- [48] Junfei Xiao, Longlong Jing, Lin Zhang, Ju He, Qi She, Zongwei Zhou, Alan Yuille, and Yingwei Li. Learning from tem-

- poral gradient for semi-supervised action recognition. In *Proceedings of the IEEE/CVF Conference on Computer Vision and Pattern Recognition*, pages 3252–3262, 2022. 1, 6, 7
- [49] Zhen Xing, Qi Dai, Han Hu, Jingjing Chen, Zuxuan Wu, and Yu-Gang Jiang. Svformer: Semi-supervised video transformer for action recognition. In *Proceedings of the IEEE/CVF Conference on Computer Vision and Pattern Recognition*, pages 18816–18826, 2023. 1, 2, 3, 6, 7, 8
- [50] Bo Xiong, Haoqi Fan, Kristen Grauman, and Christoph Feichtenhofer. Multiview pseudo-labeling for semi-supervised learning from video. In *Proceedings of the IEEE/CVF international conference on computer vision*, pages 7209–7219, 2021. 1, 2, 6
- [51] Yinghao Xu, Fangyun Wei, Xiao Sun, Ceyuan Yang, Yujun Shen, Bo Dai, Bolei Zhou, and Stephen Lin. Cross-model pseudo-labeling for semi-supervised action recognition. In *Proceedings of the IEEE/CVF Conference on Computer Vision and Pattern Recognition*, pages 2959–2968, 2022. 1, 2, 6
- [52] Taojiannan Yang, Yi Zhu, Yusheng Xie, Aston Zhang, Chen Chen, and Mu Li. Aim: Adapting image models for efficient video action recognition. *arXiv preprint arXiv:2302.03024*, 2023. 1
- [53] Sangdoon Yun, Dongyoon Han, Seong Joon Oh, Sanghyuk Chun, Junsuk Choe, and Youngjoon Yoo. Cutmix: Regularization strategy to train strong classifiers with localizable features. In *Proceedings of the IEEE/CVF international conference on computer vision*, pages 6023–6032, 2019. 1
- [54] Bowen Zhang, Yidong Wang, Wenxin Hou, Hao Wu, Jindong Wang, Manabu Okumura, and Takahiro Shinozaki. Flexmatch: Boosting semi-supervised learning with curriculum pseudo labeling. *Advances in Neural Information Processing Systems*, 34:18408–18419, 2021. 1, 2, 3, 7, 8
- [55] Hongyi Zhang, Moustapha Cisse, Yann N Dauphin, and David Lopez-Paz. mixup: Beyond empirical risk minimization. *arXiv preprint arXiv:1710.09412*, 2017. 1
- [56] Wentao Zhu. Efficient selective audio masked multimodal bottleneck transformer for audio-video classification. *arXiv preprint arXiv:2401.04154*, 2024. 1, 2